Journal of Biomechanics 147 (2023) 111455

Contents lists available at ScienceDirect

Journal of Biomechanics

journal homepage: www.elsevier.com/locate/jbiomech

Muscle inertial contributions to ankle kinetics during the swing phase of running

Jasper Verheul [a,b,*], Shinjiro Sueda [c], Sang-Hoon Yeo [b]

[a] Cardiff School of Sport and Health Sciences, Cardiff Metropolitan University, Cardiff, United Kingdom
[b] School of Sport, Exercise & Rehabilitation Sciences, University of Birmingham, Birmingham, United Kingdom
[c] Department of Computer Science and Engineering, Texas A&M University, College Station, TX, United States

ARTICLE INFO

Keywords:
Ankle kinetics
Muscle inertia
Musculoskeletal modelling
Running mechanics
Swing phase

ABSTRACT

Skeletal muscles have inertia that leads to inertial forces acting around joints. Although these inertial muscle forces contribute to joint kinetics, they are not typically accounted for in musculoskeletal models used for human movement biomechanics research. Ignoring inertial forces can lead to errors in joint kinetics, but how large these errors are in inverse dynamics calculations of common movements is yet unclear. We, therefore, examined the role of shank muscle inertia on ankle joint moments during the swing phase of running at different speeds. A custom musculoskeletal modelling and simulation platform was used to perform inverse dynamics with a model that either combined muscle mass in the total shank mass, or considered the gastrocnemius lateralis/medialis, soleus, and tibialis anterior muscles as separate masses from the shank. Ankle moments were considerably affected when muscles were modelled as separate masses, with a general shift towards reduced dorsiflexion and higher plantarflexion moments. Differences between both modelling conditions increased with running speed and ranged between 0.8 and 1.6 Nm (ankle moment profile root mean square error), 8–18 % (peak dorsiflexion moment difference) and 24–42 % (peak plantarflexion moment difference). Moreover, we observed a complex combination of inertial forces, especially those due to rotation and translation of the shank, in which the direction of inertial force changed during the swing phase. These results show that ignoring muscle inertia in musculoskeletal models can lead to under- or overestimations of structure-specific loads and thus erroneous study conclusions. Our results suggest that muscle inertial forces should be carefully considered when using musculoskeletal models.

1. Introduction

Computational models of the musculoskeletal system impact many areas of human movement science and biomechanics. Musculoskeletal modelling and simulation platforms, such as OpenSim (Seth et al., 2018) and Anybody (Damsgaard et al., 2006), allow for quantifying mechanical properties of human movement that are difficult to measure in vivo (e.g., joint reaction forces, muscle–tendon forces) and are commonly used to inform e.g., orthopaedic surgery, injury prevention, performance enhancement, or prosthetic device design. This widespread research potential thus requires musculoskeletal models and their individual components to be biologically and mechanically accurate.

Musculoskeletal models describe the multibody dynamics of a set of rigid body segments that are connected via joints. The inertia for each segment in the model combines the inertial properties of its subcomponents, e.g., muscles, tendons, and bones. This multibody system is then driven by muscle forces and corresponding joint moments. Since the muscle inertia is typically included with the total inertia of the segment they are combined with, muscles are effectively treated as inertia-less force generators. This simplification is convenient since the inertial properties of each segment can be directly estimated from cadavers or MRI imaging (Ackerman, 1998; Hanavan, 1964). Combining muscle mass and inertia with their nearest segment is, therefore, accepted as a standard method for modelling musculoskeletal systems and is implemented in most musculoskeletal modelling and simulation software (Damsgaard et al., 2006; Seth et al., 2018).

Although combining muscle mass with its nearest segment is convenient, this approach has a major limitation. A theoretical study by Pai (2010) has pointed out that a muscle's inertial forces can lead to considerable errors in joint dynamics, and that errors are nonuniform

* Corresponding author at: Cardiff Metropolitan University, Cyncoed Campus, Cyncoed Road, Cardiff CF23 6XD, United Kingdom.
E-mail address: jpverheul@cardiffmet.ac.uk (J. Verheul).

https://doi.org/10.1016/j.jbiomech.2023.111455
Accepted 13 January 2023
Available online 20 January 2023

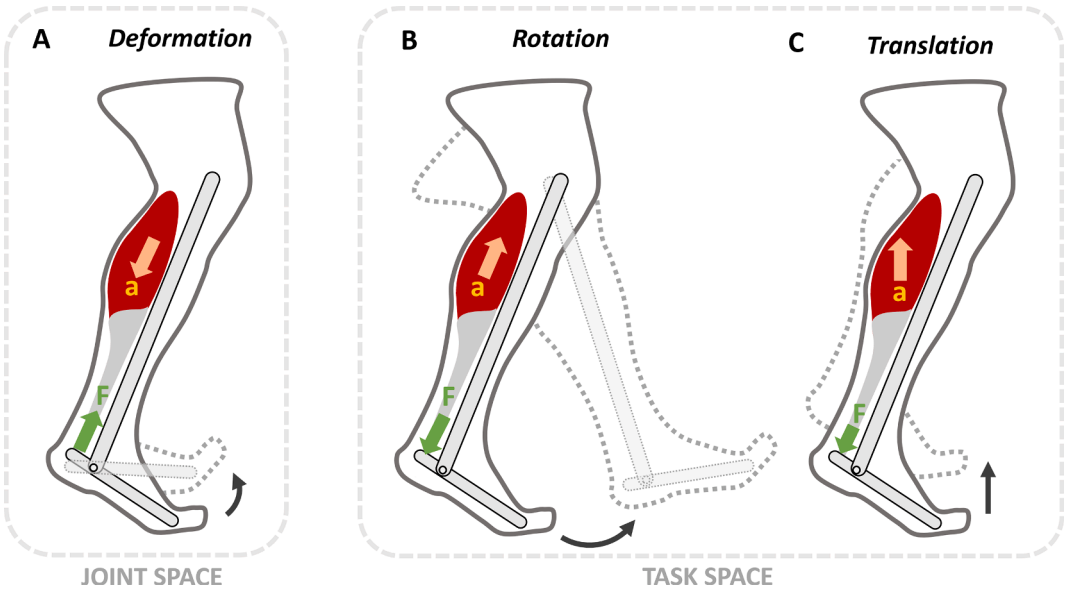

Fig. 1. A simple two-segment model of the shank and foot including a single muscle. *A*: angle changes in the joint space lead to acceleration (a) and inertial force (F) associated with muscle deformation (i.e., shortening or lengthening). *B*: rotations in the task space cause centripetal acceleration of the muscle and centrifugal force. *C*: translations in the task space cause linear muscle acceleration and inertial force.

and dependent on joint orientation (Pai, 2010). For example, we can consider a simple two-segment model of the shank and foot, with a single calf muscle crossing the ankle (Fig. 1). Ankle orientation changes in the joint space can cause deformation (i.e., lengthening or shortening) and accompanying acceleration of the muscle, which in turn leads to a force and moment acting around the ankle (Fig. 1A). Likewise, rotation and translation of the model in the task space cause centripetal and linear muscle accelerations respectively, also leading to associated forces and ankle moments (Fig. 1B-C). Moreover, it is clear from this simple example that several inertial effects can compete – that is, inertial muscle forces that occur simultaneously can cause either dorsiflexion or plantarflexion moments around the ankle. Nevertheless, it is yet unclear to what extent muscle inertial forces affect inverse dynamics analyses of common human movements, and how the distinct inertial effects contribute to changes in joint dynamics.

Running is a popular activity and widely studied movement. Human running is characterised by the absence of a double support phase (as during walking) and a distinct separation of the stance and swing phase (Novacheck, 1998). Since no considerable external forces (e.g., ground reaction forces) are acting on the leg during the swing phase, ankle kinetics is mainly determined through an interaction between muscle and inertial forces of the lower-limb segments. Hence, this allows for a direct assessment of how joint kinetics is affected by changes in lower-limb muscle inertia. In addition, lower-limb joint range of motion and segmental velocities increase considerably when running speed increases. Inertial effects of the muscles can thus be expected to be further highlighted at higher running speeds.

Except for two short phases just after and before ground contact, the ankle primarily dorsiflexes during the swing phase of running. During this phase, the tibialis anterior muscle, the primary ankle dorsiflexor, interacts with the inertial forces of the antagonistic ankle plantar flexors (i.e., gastrocnemius and soleus), which account for almost 70 % of the shank mass (Ward et al., 2009). It is, therefore, reasonable to assume that changes in ankle kinetics due to calf muscle inertia directly affect the force demands of an individual muscle, i.e., tibialis anterior. For this reason, the primary goal of this study was to examine the effects of shank muscle inertia on ankle kinetics during the swing phase of running. In addition, we aimed to identify the distinct contributions of various inertial effects to the differences in ankle kinetics.

2. Methods

2.1. Data

Data was collected for one healthy youth-academy footballer (male, 19 yrs, 185 cm, 76.3 kg). The participant provided informed consent before data collection, following Liverpool John Moores University ethics regulations. After a warmup consisting of easy running and familiarisation on the treadmill, the participant performed two consecutive running trials on a motorised treadmill (Woodway Pro, Woodway UK) at four different speeds of 10, 13, 17, and 19.1 km•h^{-1}.

During treadmill running, kinematic data of the lower limbs and pelvis were captured using a 38 *retro*-reflective marker set. Markers were attached to the left and right anterior/posterior superior iliac spine, femur greater trochanter, medial/lateral femoral epicondyle, medial/lateral malleolus, calcaneus, first and fifth metatarsus head, and the tip of the foot, together with four-marker cluster plates on the right and left shank and tibia. Three-dimensional marker trajectories were recorded for ten seconds during each trial with eight infrared cameras (Qqus 300+, Qualisys) sampling at 250 Hz, using Qualisys Track Manager Software (QTM v.2018, Qualisys). In addition, a static calibration trial was recorded to scale the dimensions of a generic musculoskeletal model to the participant.

2.2. Modelling and analyses

Marker trajectories were filtered with a 4th-order Butterworth filter at 15 Hz and exported to OpenSim v.4.3 (Seth et al., 2018). The skeletal structure of the Rajagopal model (Delp et al., 1990; Rajagopal et al., 2016) was used and modified by removing the torso and head segments, restricting the knee to flexion/extension and avoiding knee translation, making the ankle a one-degree-of-freedom joint between the tibia and talus (dorsiflexion/plantarflexion), and fixating the subtalar and metatarsal-phalangeal joints to assume a rigid foot (Fig. 2). The model was scaled to the participant's dimensions using the static calibration trial. OpenSim's Inverse Kinematics and Dynamics Tools were used to determine lower-limb kinematics and kinetics respectively. Segment and joint kinematics and kinetics data were exported to MATLAB (v. R2021a, MathWorks) for further analysis.

Lower-limb kinematics and segmental properties (mass, centre of

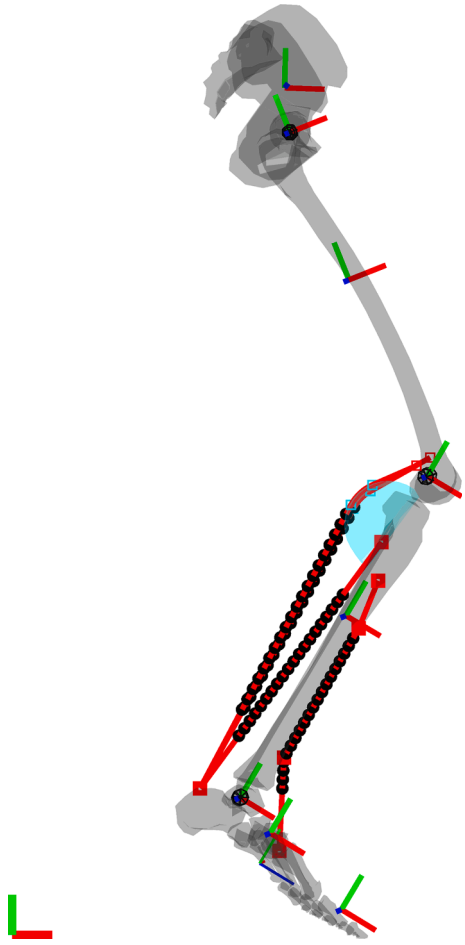

Fig. 2. Twenty discrete mass points were distributed along the muscle paths of the tibialis anterior, soleus, and gastrocnemius medialis and lateralis. Red (anteroposterior), green (vertical), and blue (mediolateral) axes represent the centre of mass coordinate systems for each segment. (For interpretation of the references to colour in this figure legend, the reader is referred to the web version of this article.)

mass, inertia) of the Rajagopal model were used as input to RedMax – a custom MATLAB-based musculoskeletal modelling and simulation tool used in robotics and computer graphics (Wang et al., 2022, 2019; Xu et al., 2021). RedMax was used to perform inverse dynamics, either with muscle masses included in the combined shank mass (CSM) or modelled as separate muscle masses (SMM). For SMM, the total mass of the shank segment (3.76 kg) was divided between the muscles as follows: tibialis anterior (12.1 %; 0.45 kg), soleus (41.5 %; 1.56 kg), gastrocnemius medialis (17.1 %; 0.64 kg) and lateralis (9.4 % 0.35 kg), and the tibia bone plus remaining muscles and connective tissues (20 %; 0.75 kg), based on cadaver data (Ward et al., 2009). Muscle insertion points on the thigh, shank and foot segments, and muscle wrapping surfaces and via points, were as defined by Rajagopal et al. (2016). All muscle–tendon unit mass was assumed to be from the muscle and not the tendon. For each muscle–tendon unit, the tendon length (taken from Rajagopal et al. (2016)) was divided into two equal lengths and assigned as the origin and insertion tendon length of the muscle–tendon path. The tibialis anterior was modelled as a polyline muscle passing through two path points, the soleus was modelled as a straight-line muscle, and the two gastrocnemius muscles were modelled as wrapped muscles with a cylinder. Twenty discrete muscle-mass points were distributed uniformly along the remaining length of each muscle, considering wrapping surfaces and via points (Fig. 2).

The inertial contributions of the muscle-mass points were added as follows. Each mass point moved kinematically along their respective muscle–tendon unit paths, as a function of the generalized coordinate values. Starting with the standard equations of motion for the r degrees of freedom of the skeletal joints, $M_s\ddot{q} = f_s$, (where M_s is the inertia, and f_s are the gravity and Coriolis forces of the skeleton), the generalized inertia and the generalized force were augmented as:

$$\left(M_s + J^T M_a J\right)\ddot{q} = f_s + J^T\left(f_a - M_a \dot{J}\dot{q}\right) \tag{1}$$

in which M_a is the $3n \times 3n$ inertia tensor of the muscles with n being the total number of discrete mass points ($n = 20$), f_a is the $3n \times 1$ force vector acting on the muscles due to gravity, and J is the $3n \times r$ Jacobian matrix that converts the joint velocities to muscle mass velocities. Further details and an in-depth derivation of the equations of motion can be found in Wang et al. (2022).

Ankle moments computed with CSM in RedMax were validated against those from OpenSim. Ankle moments were filtered at 6 Hz. Individual swing phases of the right leg were cut from the ten-second trials between takeoff and touchdown, which were determined as the maximal knee extension angle (Fellin et al., 2010) and minimal vertical velocity of the pelvis centre of mass (Milner and Paquette, 2015), respectively. To compare RedMax and OpenSim, a Bland-Altman analysis (Bland and Altman, 2010) was used to assess the bias (mean difference) and 95 % limits of agreement (±2 standard deviations) between the calculated ankle moments, and root mean square errors (RMSE) were calculated.

2.3. Muscle-inertia effects

To examine the impact of muscle inertia, ankle moments calculated with CSM and SMM (both using RedMax) were compared using Bland-Altman analysis and by calculating curve RMSE. Furthermore, the difference in peak dorsiflexion and plantarflexion moments during the swing phase was determined and evaluated using a two-way repeated measures ANOVA. Significance was accepted when $p < 0.05$. Effect sizes were determined by calculating the partial Eta squared (η_p^2) and applying Cohen's rules of thumb (0.01 = small, 0.06 = medium, 0.14 = large) (Cohen, 1988). Statistical analyses were performed with SPSS (v.27, IBM).

For further analysis, the acceleration vector of each muscle-mass point was decomposed into axial and orthogonal components, based on the assumption that only the axial component of the inertial force can be transmitted to bones and thus contribute to the joint moment. The total world accelerations of the muscle mass points, a^{total}, were computed by applying finite differencing to the world velocity values of the mass points in RedMax (note: RedMax works at the velocity level). Axial acceleration a_{ax}^{total} was defined as the acceleration along the tangent direction at each muscle-mass point (Fig. 2). The total inertial force contribution of each muscle to the change in joint moments between CSM and SMM was then determined according to:

$$F_M^{total} = \sum_{i=1}^{20} m^i \bullet \left(a_{ax}^{total}\right)^i \tag{2}$$

in which F_M^{total} is the total inertial muscle force of muscle M due to the acceleration of each muscle-mass point i, and m and a_{ax}^{total} are the mass and axial acceleration of each mass point respectively.

To evaluate the distinct inertial effects in the joint and task space, mass point accelerations were further separated into accelerations *moving with* the shank, and accelerations *relative to* the shank. For each time step, the accelerations of the muscle-mass points *moving with* the shank (a^{fixed}) were obtained by temporarily assuming the mass points to be rigidly attached to the shank, after which their acceleration vectors were computed using the shank's spatial acceleration:

$$\left(a^{fixed}\right)^i = \left(J^{fixed}\ddot{q} + \dot{J}^{fixed}\dot{q}\right)^i \tag{3}$$

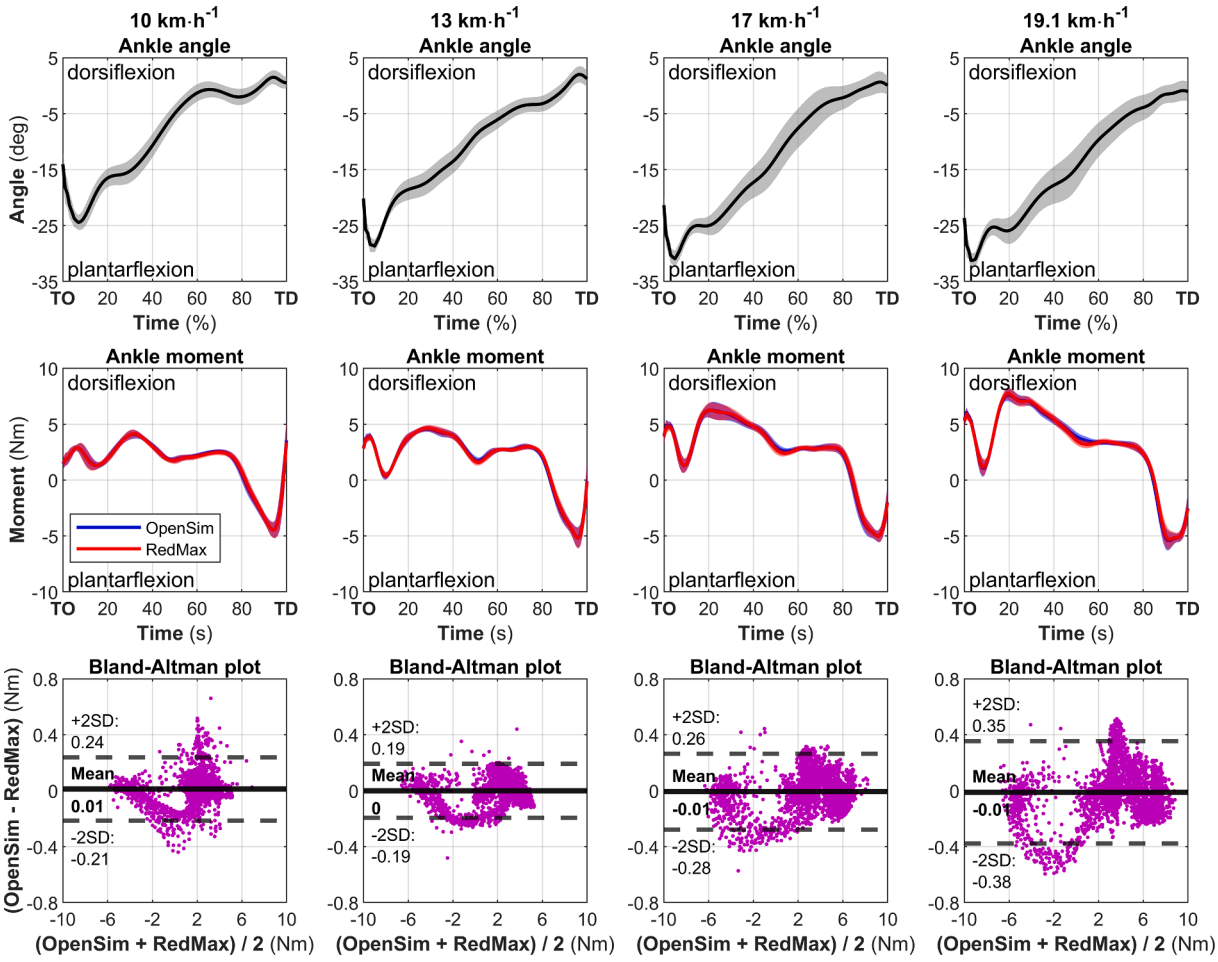

Fig. 3. Mean ± standard deviation ankle angle (top row) and moment (middle row) profiles during the swing phase of running at four different speeds. Ankle moments in the middle row were calculated in OpenSim (blue) and RedMax (red) using a combined shank mass (CSM) – note that these are two separate curves that are superimposed. Bland-Altman plots (bottom row) showed low bias (mean difference; black solid horizontal lines) and limits of agreement (mean ± two standard deviations, black dashed horizontal lines). *TO* = take off; *TD* = touch down; *SD* = standard deviation. (For interpretation of the references to colour in this figure legend, the reader is referred to the web version of this article.)

in which J^{fixed} is the Jacobian that maps the joint angles to the muscle points assuming that they are rigidly fixed to the segment. The accelerations of these points were then projected onto the axial direction vector as before, and the resulting axial accelerations, a_{ax}^{fixed}, were used to calculate the associated inertial force F_M^{fixed} for each muscle.

$$F_M^{fixed} = \sum_{i=1}^{20} m^i \bullet \left(a_{ax}^{fixed}\right)^i. \tag{4}$$

Finally, F_M^{fixed} was subtracted from the total inertial muscle force F_M^{total} to get the inertial forces associated with the muscle-mass points accelerating *relative to* the shank ($F_M^{relative}$).

$$F_M^{relative} = F_M^{total} - F_M^{fixed}. \tag{5}$$

3. Results

A total of 24 (10 km•h^{-1}), 24 (13 km•h^{-1}), 27 (17 km•h^{-1}), and 27 (19.1 km•h^{-1}) swing phases for the right leg were identified from the two ten-second trials per speed and included in the analysis. Ankle angle and moment (calculated with CSM) profiles for each running speed are shown in Fig. 3. Ankle range of motion was between 30° plantarflexion and 3.5° dorsiflexion across the four running speeds. There was a very high agreement between ankle moments calculated in OpenSim and RedMax, with mean differences ranging between −0.01 and 0.01 Nm across all running speeds. The highest 95 % limits of agreement were between −0.38 and 0.35 Nm at the highest running speed (Fig. 3). Between-software RMSE for the ankle moment profiles was 0.1 ± 0.1 Nm (10 km•h^{-1}), 0.1 ± 0 Nm (13 km•h^{-1}), 0.1 ± 0 Nm (17 km•h^{-1}), and 0.2 ± 0 Nm (19.1 km•h^{-1}).

After confirming that the inverse dynamics analysis results from RedMax and OpenSim are in close agreement for CSM, the effect of modelling muscles as SMM was examined. Modelling the four major shank muscles as SMM considerably decreased (dorsiflexion) or increased (plantarflexion) ankle joint moments during the different parts of the swing phase (Fig. 4). There was a positive bias (i.e., CSM > SMM) increasing from 0.6 Nm at 10 km•h^{-1} to 0.95 Nm at 19.1 km•h^{-1}. Moreover, limits of agreement increased with speed from −0.31–1.52 Nm (10 km•h^{-1}), −0.82–2.16 Nm (13 km•h^{-1}), −1.25–2.91 Nm (17 km•h^{-1}), to −1.63–3.52 (19.1 km•h^{-1}).

RMSE between ankle moment profiles calculated with CSM and SMM increased with running speed from 0.8 Nm (10 km•h^{-1}) to 1.6 (19.1 km•h^{-1}). Differences in peak moments between CSM and SMM were also more pronounced with increasing running speed (Fig. 5) and ranged from 8 to 18 % (dorsiflexion) and 24–42 % (plantarflexion). For peak dorsiflexion moment, there were significant main effects ($p < 0.001$) with large effect sizes for muscle modelling condition ($\eta_p^2 = 0.96$) and running speed ($\eta_p^2 = 0.9$), and a significant interaction between modelling condition and speed ($p < 0.001$; $\eta_p^2 = 0.56$). For peak plantarflexion moment, there also were significant main effects ($p < 0.001$) with large

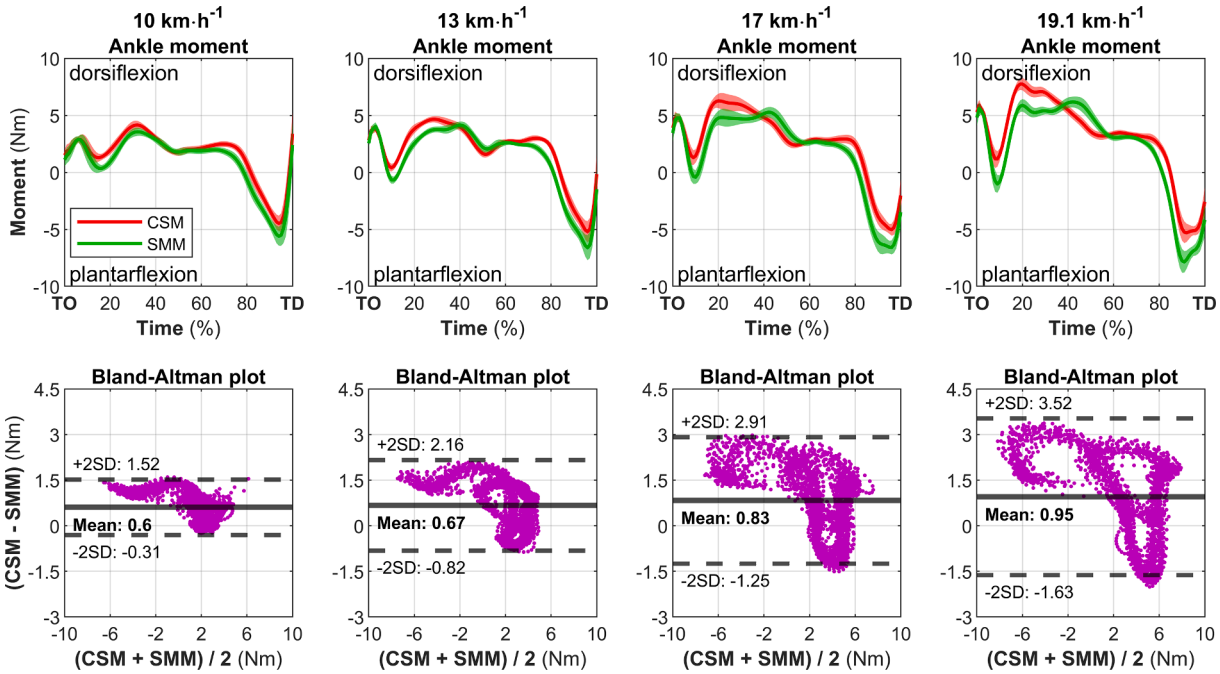

Fig. 4. *Top row*: Mean ± standard deviation ankle moment profiles during the swing phase of running at four different speeds. Ankle moments were calculated in RedMax with a combined shank mass (CSM; red) or separate muscle masses (SMM; yellow). *Bottom row*: Bland-Altman plots including bias (mean difference; black solid horizontal lines) and limits of agreement (black dashed horizontal lines). *TO* = take off; *TD* = touch down; *SD* = standard deviation. (For interpretation of the references to colour in this figure legend, the reader is referred to the web version of this article.)

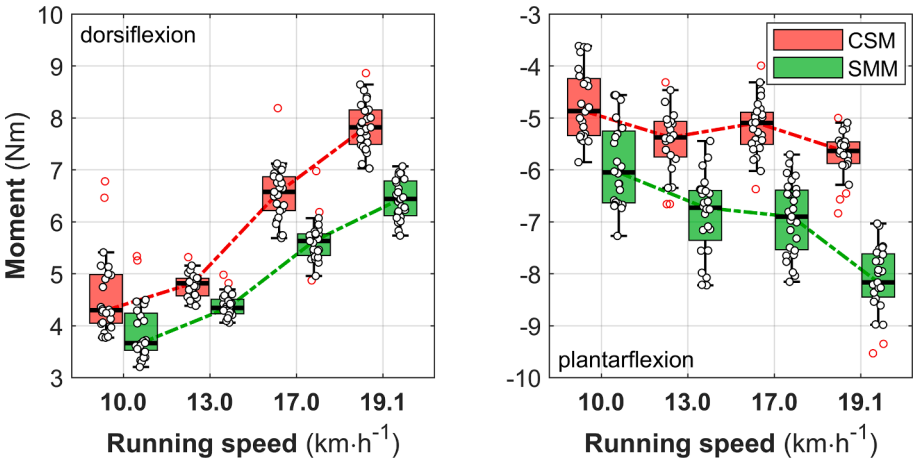

Fig. 5. Peak dorsiflexion (left) and plantarflexion (right) moments, calculated with a combined shank mass (CSM; red) or separate muscle masses (SMM; green), at four different running speeds. (For interpretation of the references to colour in this figure legend, the reader is referred to the web version of this article.)

effect sizes for muscle modelling condition ($\eta_p^2 = 0.99$) and running speed ($\eta_p^2 = 0.53$), and a significant interaction between modelling condition and speed ($p < 0.001$; $\eta_p^2 = 0.73$).

After establishing the ankle moment differences between CSM and SMM, each muscle's inertial force contribution to these differences was analysed (Eqs. (2)–(5); Fig. 6). Most inertial muscle forces were associated with the accelerations moving with the shank due to rotation and translation in the task space (Fig. 6, middle row). In contrast, only a small part of the inertial forces was associated with muscle-mass point accelerations relative to the shank, due to ankle angle changes in the joint space (Fig. 6, bottom row). Most of these relative inertial muscle forces, especially for the soleus, occurred during the first 10 % of the swing phase.

4. Discussion

This study shows the impact of shank muscle inertia on ankle kinetics during running. Our results reveal that shank muscle inertia either reduces (dorsiflexion) or enlarges (plantarflexion) ankle moments, during different parts of the swing phase. To the best of our knowledge, this is the first study to demonstrate muscle-inertia effects on inverse dynamics analysis of a common human movement.

When muscle inertia was considered, we found a general decrease in dorsiflexion moments throughout the swing phase, except during mid-swing. Since shank muscle inertia was the only difference between CSM and SMM, these findings need to be explained by considering the different inertial forces, which can counter each other. There are two main components of inertia to consider during the swing phase of running (Fig. 1). First, there are inertial forces associated with muscle

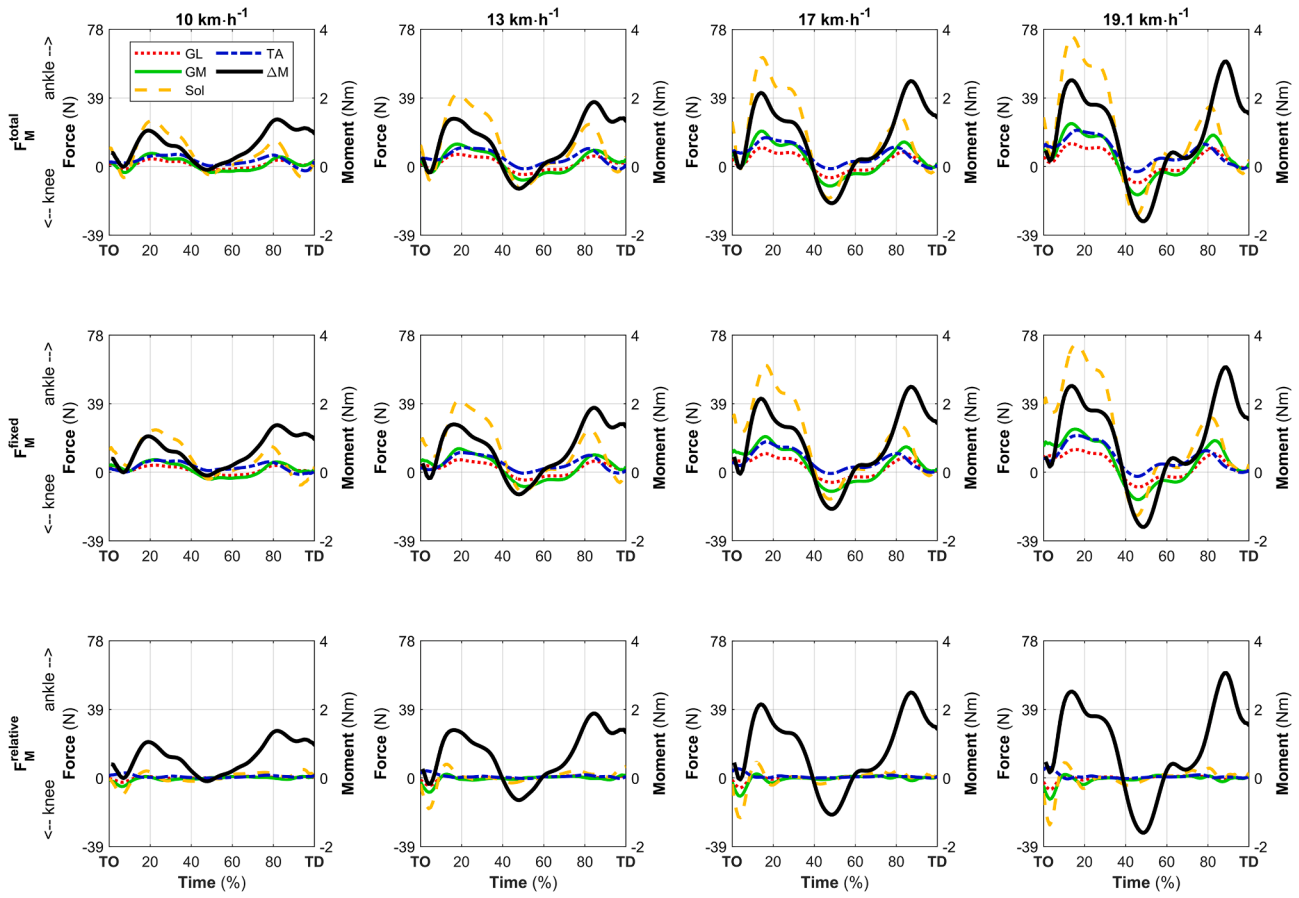

Fig. 6. Inertial forces for each of the four muscles included in the model (left y-axis) and the difference in ankle moments between CSM and SMM (right y-axis). Positive forces work towards the ankle and negative forces work towards the knee. *Top row*: inertial force F_M^{total} due to the total axial muscle-mass point accelerations. *Middle row*: inertial force F_M^{fixed} due to muscle-mass point accelerations moving with the shank. *Bottom row*: inertial force $F_M^{relative}$ due to muscle-mass point accelerations relative to the shank (i.e., the middle row subtracted from the top row). *GL* = gastrocnemius lateralis; *GM* = gastrocnemius medialis; *Sol* = soleus; *TA* = tibialis anterior; *ΔM* = ankle moment difference between models (i.e., $M_{CSM} - M_{SMM}$); *TO* = take off; *TD* = touch down.

deformation (lengthening and shortening). For example, ankle dorsiflexion lengthens the calf muscles, which causes inertial forces that work towards the knee and increase the resistance against dorsiflexion. We found that these forces are primarily present during early swing (Fig. 6, bottom row) when the ankle rapidly plantarflexes (Fig. 3) and the calf muscles shorten. This calf muscle shortening leads to inertial forces working towards the knee and therefore increases resistance against dorsiflexion and required dorsiflexion moments. Second, there are centrifugal forces caused by the leg segments swinging backwards and forward (Fig. 1B). For the calf muscles, the centrifugal force works towards the ankle when the shank swings forward and decreases resistance against dorsiflexion. This backward/forward shank acceleration is substantial during the first and last ~ 40 % of the swing phase, but much smaller or even negative during mid-swing. It is clear from Fig. 6 that centrifugal forces counter the inertial forces associated with muscle shortening during the early swing phase. More importantly, our results show that the centrifugal effect is the dominant contributor to ankle moments during movement. Muscle inertia is therefore primarily to be considered during rapid movements with high segmental accelerations.

The soleus muscle was the largest contributor to the differences in ankle joint moments (Fig. 6). A key reason for this is that the mass of the soleus is the largest (1.56 kg) of the four muscles included in our model and inertial muscle forces are linearly related to muscle mass. In addition, the soleus is a monoarticular muscle of which the inertial forces are affected by the movement of the ankle only, whereas the inertial forces of the biarticular gastrocnemius muscles are affected by both ankle and knee movement. Especially during the late swing phase, the knee primarily extends and pulls the gastrocnemius muscle masses towards the knee. This may have counteracted the centrifugal inertial force toward the ankle, and therefore resulted in a smaller inertial contribution of the gastrocnemius to the ankle moment compared to that of the soleus.

Since it is commonly assumed in muscle mechanics that muscles cannot push, one can question if inertial forces toward the ankle affect ankle kinetics. In a *passive* musculoskeletal system, inertial forces toward the insertion point are likely to buckle the tendon and connective tissues and should therefore not be transmitted to ankle moments. However, we expect that inertial force can indeed affect ankle kinetics in an *active* musculoskeletal system, such as the one examined in this study. During running, most ankle controllers retain at least 10 % of their maximum activation level throughout the swing phase (Reber et al., 1993). This indicates that a reasonable amount of co-contraction and muscle forces around the ankle persists during swing. Given these baseline muscle forces due to co-contraction, it is likely that the inertial force toward the ankle can reduce the existing contractile force towards the knee, but not change its direction. This invites an interesting further investigation to examine if such reductions do exist and can be measured in *in vivo* experiments.

Since the tibialis anterior is the primary dorsiflexor of the ankle, it is reasonable to assume that changes in ankle dorsiflexion moment directly affect the tibialis anterior force demands. Hence, we examined ankle kinetics during the swing phase of running to isolate the effect of (calf) muscle inertia on an individual muscle. Peak dorsiflexion moment reductions of up to 18 % during early swing suggest that required tibialis

anterior forces can be considerably overestimated when using CSM. In addition, CSM's underestimation of the dorsiflexion moment during mid-swing (especially at higher running speeds; Fig. 4) suggests that the tibialis anterior is generally required to produce consistent force throughout the swing phase of running. This can explain the overall high level of tibialis anterior activation observed during this phase (Novacheck, 1998; Reber et al., 1993). These errors can have important implications for investigations of running-related injuries that are associated with tibialis anterior fatigue and overuse, such as chronic exertional compartment syndrome (Franklyn-Miller et al., 2014), medial tibial stress syndrome (Hamstra-Wright et al., 2015), and tibialis anterior muscle pain. Likewise, many other structure-specific load metrics can be considerably over- or underestimated by ignoring muscle inertia in inverse dynamics calculations, which in turn can lead to erroneous study conclusions. Furthermore, errors can be more severe for high-velocity movements (as discussed above), joints crossed by more biarticular muscles (Pai, 2010) (e.g., the hip), and muscles with large masses (e.g., the quadriceps). We, therefore, recommend that human movement scientists and biomechanics researchers carefully consider the role of muscle inertia on inverse dynamics calculations during movement.

Our results reveal a considerable impact of muscle inertia on joint kinetics during running. An important question is therefore how muscle inertia should be accounted for in musculoskeletal models used for human movement biomechanics research. Several options have been suggested previously (Pai, 2010): not changing anything, adding mass to existing muscle models (e.g., (Ross and Wakeling, 2016)), calculating each muscle's mass contribution to joint inertia (as in this study), or using continuum-mechanics based muscle models (such as finite element models). Each of these solutions comes with benefits and disadvantages that are study-dependent and should be carefully weighed by the investigator. For example, muscle inertia is likely to impact joint kinetics less for slow movements, monoarticular muscles, and small muscle masses. One may therefore choose to prefer the convenience of existing approaches that use CSM in such cases. Likewise, added model complexity can substantially increase computational cost which can be an unfeasible option for large-scale investigations. Perhaps the most important consideration is that most human movement biomechanics researchers rely on existing models from openly available musculoskeletal modelling and simulation software (e.g., OpenSim, AnyBody). Widespread consideration of the impact of muscle inertia in human movement biomechanics is therefore likely dependent on future implementations of mass properties in commonly used phenomenological muscle models (i.e., Hill-type models (Zajac, 1989)) or of each muscle's contribution to the joint inertia within existing software.

The magnitude of the impact of muscle inertia on joint kinetics, as demonstrated in this study, is dependent on several muscle–tendon parameters. In our study, these parameters, such as the total amount of segmental mass assigned to the muscles or the distribution of the tendon length on each side of the muscle–tendon unit, were based on normative cadaver measurement (Ward et al 2009) and scaled to the participant's dimensions. However, since muscle–tendon characteristics vary between different individuals and muscles (and even change during movement), using person-specific parameters (e.g., from DXA scans or ultrasonographic measurements) could increase accuracy. We, therefore, conducted an additional sensitivity analysis on three representative muscle–tendon parameters (the total shank mass assigned to the muscles, the number of muscle mass points used for each muscle, and the distribution of the total tendon length on each side of the muscle–tendon unit) to evaluate how much the inertial effect on ankle kinetics is affected by the chosen parameters (see Appendix A for details). This sensitivity analysis confirmed that, within physiologically realistic ranges, the inertial effect is only minimally affected by those parameters. This suggests that the use of normative muscle–tendon properties is sufficient to reliably estimate the inertial effect of lower-limb muscles on ankle kinetics. Nevertheless, future studies may seek to establish the magnitude of inertial effects in different individuals – e.g., those with a higher BMI (and associated fat mass) may show further increases in inertial muscle forces and thus larger errors in joint moments.

Several considerations related to the modelling choices made in this study, and the interpretation of our results, need to be highlighted. These considerations are primarily related to the use of discretely sampled muscle-mass points, the relatively small ankle moments during the swing phase of running compared to the stance phase, the foot-strike pattern adopted during running, the rigid foot segment used in our model, and the magnitude of the observed joint moment differences. We discuss these in more detail in Appendix B.

5. Conclusions

This study demonstrates for the first time that muscle inertia has a considerable impact on joint kinetics during a commonly studied human movement. Our results reveal that shank muscle inertia reduces ankle dorsiflexion moments and increases plantarflexion moments during the swing phase of running. Over- or underestimations of these and other structure-specific loads (e.g., muscle–tendon forces, joint reaction forces) can lead to erroneous conclusions in studies that rely on musculoskeletal models that do not account for muscle inertia. These findings suggest that the role of muscle inertia on inverse dynamics calculations should be carefully considered in human movement science and biomechanics research.

CRediT authorship contribution statement

Jasper Verheul: Writing – review & editing, Writing – original draft, Visualization, Validation, Supervision, Software, Resources, Project administration, Methodology, Investigation, Formal analysis, Data curation, Conceptualization. **Shinjiro Sueda:** Writing – review & editing, Visualization, Validation, Supervision, Software, Resources, Project administration, Methodology, Investigation, Formal analysis, Data curation, Conceptualization, Writing – original draft. **Sang-Hoon Yeo:** Writing – review & editing, Visualization, Validation, Supervision, Resources, Project administration, Methodology, Investigation, Formal analysis, Data curation, Conceptualization, Writing – original draft.

Declaration of Competing Interest

The authors declare that they have no known competing financial interests or personal relationships that could have appeared to influence the work reported in this paper.

Acknowledgement

The authors acknowledge the Biotechnology and Biological Sciences Research Council (BB/S003762/1) and The National Science Foundation (CAREER-1846368) for financially supporting this work.

Appendix A. Muscle modelling parameter sensitivity.

Aim

Muscle inertial effects were investigated by including four shank muscles in a lower-limb model and examining the changes in ankle joint moments during the swing phase of running. Inertial effects are therefore dependent on several assumptions and modelling choices for the four muscles included in the model, such as the assumed mass (distribution) and tendon lengths of each muscle. These parameters were chosen to represent physiologically realistic values based on previous research (see main methods section) but can likely vary between different individuals and muscles. Although the use of generic modelling parameters is desirable, the magnitude of muscle inertial effects on joint kinetics may be sensitive to slight variations in the chosen parameters. The aim of this appendix was, therefore, to examine the sensitivity of

inertial effects to three important muscle modelling parameters: 1) the total mass assigned to the four shank muscles, 2) the number of muscle mass points used for each muscle, and 3) the distribution of the total tendon length on each side of the muscle–tendon unit.

Methods

Methodologies for investigating the sensitivity of our results to muscle modelling parameter choices were identical to those described in the methods section of the main manuscript. Three muscle modelling parameters were individually altered. Where relevant the parameters were kept within a physiologically realistic range. First, a total of either 70 %, 80 %, or 90 % of the total shank mass was distributed between the four shank muscles, to examine the impact of the total muscle mass relative to the combined shank mass (CSM). For each mass distribution the centre of mass of the segment was unchanged. Second, a total of 10, 20, or 30 mass points were distributed uniformly along the length of the muscle, to examine the impact of the number of muscle mass points used. Third, tendon lengths were divided as 50–50 %, 40–60 %, or 30–70 % (proximal–distal), to examine the distribution of the total tendon length on each side of the muscle–tendon unit. Inverse dynamics was performed in RedMax. Ankle joint moments during the swing phase were qualitatively compared to the model with CSM (i.e., no separate muscle masses were modelled) through visual inspection.

Results

See Figs. A1-A3.

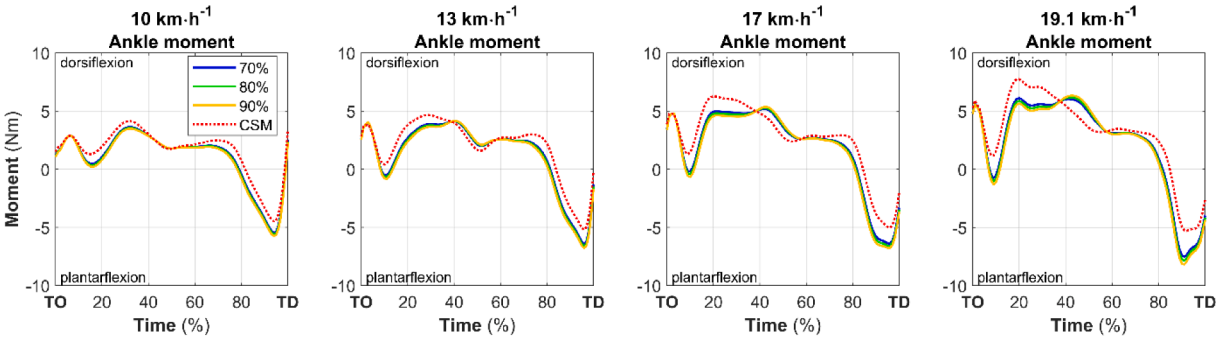

Fig. A1. Mean ankle moment profiles during the swing phase of running at four different speeds. The shank mass was modelled as either a combined shank mass (CSM; red solid line), or with a total of 70% (blue dashed line), 80% (green dashed line), or 90% (yellow dashed line) of the total shank mass assigned to the four muscles.

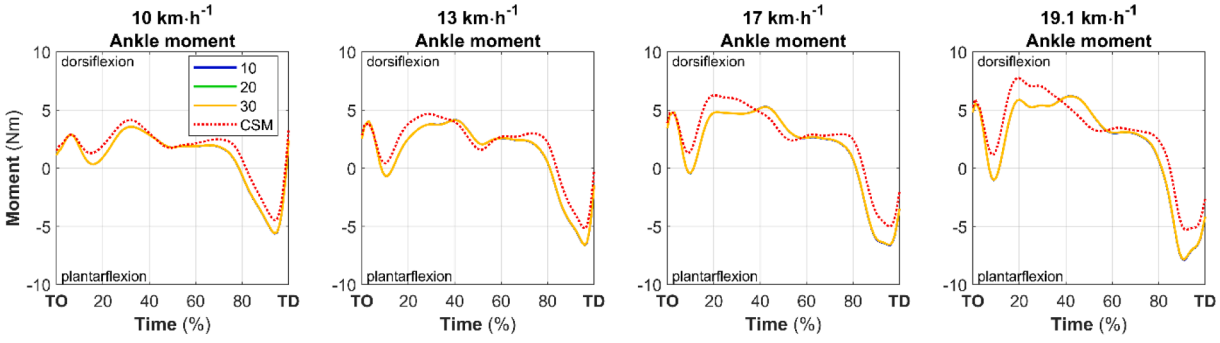

Fig. A2. Mean ankle moment profiles during the swing phase of running at four different speeds. Each muscle's mass was uniformly distributed along its length using either 10 (blue dashed line), 20 (green dashed line), or 30 (yellow dashed line) muscle mass points. *CSM* = combined shank mass (red solid line).

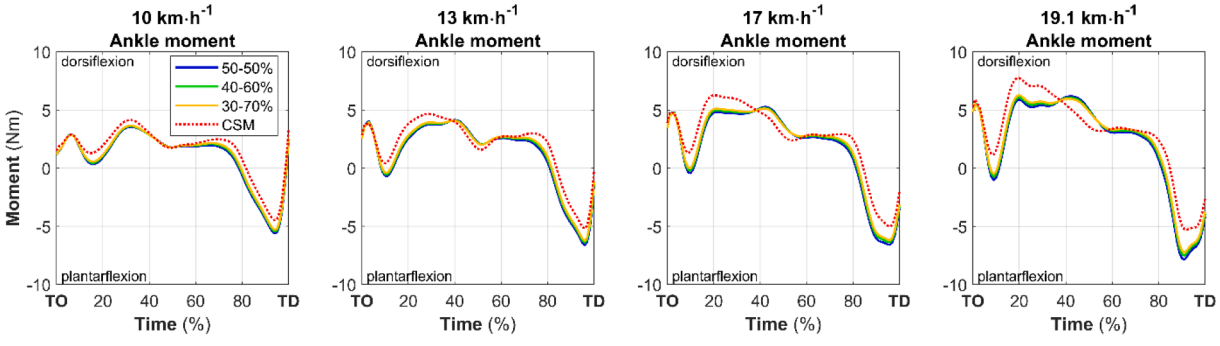

Fig. A3. Mean ankle moment profiles during the swing phase of running at four different speeds. The total tendon length was divided between both sides of the muscle as 50–50 % (blue dashed line), 40–60 % (green dashed line), or 30 (yellow dashed line) muscle mass points. *CSM* = combined shank mass (red solid line).

Conclusions

Ankle joint moments were affected minimally when three important muscle modelling parameters were altered within a physiologically realistic range. Hence, the contribution of muscle inertia on joint kinetics is only minimally sensitive to moderate variations in the total mass assigned to the four shank muscles, the number of muscle mass points used for each muscle, and the distribution of the total tendon length on each side of the muscle–tendon unit. Using normative muscle–tendon properties is thus sufficient to reliably estimate the inertial effect of lower-limb muscles on ankle kinetics.

Appendix B. Study considerations

Several considerations related to the modelling choices made in this study, and the interpretation of our results, need to be highlighted.

First, for reasons of simplicity we used discretely sampled muscle-mass points. Although the number of mass points did not affect our results (as shown in Appendix A), this method does not consider the muscle's volumetric shape. A shape-varying method in which parts of the muscle–tendon unit contract differently over its lengths has been described (Han et al., 2015), but cannot be used for muscle paths that involve wrapping surfaces and via points, such as those in commonly used musculoskeletal models. Combining both aspects could further refine muscle inertial contributions to joint kinetics.

Second, ankle moments during the swing phase of running are relatively small compared to the stance phase (Novacheck, 1998). One could argue that larger joint moments associated with the stance phase are more relevant e.g., for injury prevention. However, other factors that contribute to ankle kinetics during stance, such as the external ground reaction forces, can introduce an additional source of joint-moment variability. This makes it difficult to isolate the effects of muscle inertia, as was the aim of this study. Moreover, since segmental accelerations can be high during landing, we expect our findings to extend (and possibly be magnified) to the stance phase.

Third, the participant in this study ran with a clear heel-strike landing. Changes in ankle kinetics may be smaller for habitual forefoot runners or during sprinting. Nevertheless, this does not diminish the demonstrated effects of muscle inertia on inverse dynamics calculations, especially when extended to other joints and muscles.

Fourth, we assumed a rigid foot segment for reasons of simplicity and because four markers placed on the outside of the shoe (as used in this study) are typically insufficient to describe the kinematics of the metatarsophalangeal joint well. Fixing the metatarsophalangeal joint could have a minor effect on the ankle joint moment. However, since we used the same rigid foot segment for all running speeds and both conditions (i.e., CSM and SMM) we do not expect that the use of a non-rigid foot alters the inertial force effects on ankle kinetics that we observed.

Finally, the magnitude of the observed joint moment differences in this study should be considered. Assuming a moment arm of 40 mm for the tibialis anterior (Maganaris, 2000) or Achilles tendon (Rasske et al., 2017), a 4 Nm change in ankle moment leads to a difference in required muscle force of 100 N (~0.13 BW). Given that the total load on the Achilles tendon is ~ 5–7 BW during the stance phase of running (Demangeot et al., 2023), one could argue that the effect on individual muscle demands is relatively small and insignificant. We would, however, point out that inertial effects are likely to be further magnified during the stance phase due to higher accelerations (as discussed above), and at joints that involve more muscles (e.g., the knee). Nevertheless, the value of increased accuracy should be weighed up against the additional efforts of modelling muscle inertia.

References

Ackerman, M.J., 1998. The visible human project. Proc. IEEE 86, 504–511. https://doi.org/10.1109/5.662875.

Bland, J.M., Altman, D.G., 2010. Statistical methods for assessing agreement between two methods of clinical measurement. Int. J. Nurs. Stud. 47, 931–936. https://doi.org/10.1016/j.ijnurstu.2009.10.001.

Cohen, J., 1988. Statistical power analysis for the behavioral sciences, second ed. Erlbaum, Hillsdale.

Damsgaard, M., Rasmussen, J., Christensen, S.T., Surma, E., de Zee, M., 2006. Analysis of musculoskeletal systems in the AnyBody Modeling System. Simul. Model. Pract. Theory 14, 1100–1111. https://doi.org/10.1016/j.simpat.2006.09.001.

Delp, S.L., Loan, J.P., Hoy, M.G., Zajac, F.E., Topp, E.L., Rosen, J.M., 1990. An interactive graphics-based model of the lower extremity to study orthopaedic surgical procedures. IEEE Trans. Biomed. Eng. doi 37 (8), 757–767.

Demangeot, Y., Whiteley, R., Gremeaux, V., Degache, F., 2023. The load borne by the Achilles tendon during exercise: a systematic review of normative values. Scandinavian Med Sci Sports 33 (2), 110–126.

Fellin, R.E., Rose, W.C., Royer, T.D., Davis, I.S., 2010. Comparison of methods for kinematic identification of footstrike and toe-off during overground and treadmill running. J. Sci. Med. Sport 13, 646–650. https://doi.org/10.1016/j.jsams.2010.03.006.

Franklyn-Miller, A., Roberts, A., Hulse, D., Foster, J., 2014. Biomechanical overload syndrome: defining a new diagnosis. Br. J. Sports Med. 48, 415–416. https://doi.org/10.1136/bjsports-2012-091241.

Hamstra-Wright, K.L., Huxel Bliven, K.C., Bay, C., 2015. Risk factors for medial tibial stress syndrome in physically active individuals such as runners and military personnel: a systematic review and meta-analysis. Br. J. Sports Med. 49, 362–369. https://doi.org/10.1136/bjsports-2013-093262.

Han, M., Hong, J., Park, F.C., 2015. Musculoskeletal dynamics simulation using shape-varying muscle mass models. Multibody Syst. Dyn. 33, 367–388. https://doi.org/10.1007/s11044-014-9427-6.

Hanavan, E.P., 1964. A mathematical model of the human body. WADC Tech. Rep. AMRL-TR-64-102, Aerosp. Med. Researsch Lab. Wright-Patterson Air Force Base, OH.

Maganaris, C.N., 2000. In vivo measurement-based estimations of the moment arm in the human tibialis anterior muscle-tendon unit. J. Biomech. 33, 375–379. https://doi.org/10.1016/S0021-9290(99)00188-8.

Milner, C.E., Paquette, M.R., 2015. A kinematic method to detect foot contact during running for all foot strike patterns. J. Biomech. 48, 3502–3505. https://doi.org/10.1016/j.jbiomech.2015.07.036.

Novacheck, T.F., 1998. The biomechanics of running. Gait Posture 7 (1), 77–95.

Pai, D.K., 2010. Muscle mass in musculoskeletal models. J. Biomech. 43, 2093–2098. https://doi.org/10.1016/j.jbiomech.2010.04.004.

Rajagopal, A., Dembia, C.L., DeMers, M.S., Delp, D.D., Hicks, J.L., Delp, S.L., 2016. Full-Body musculoskeletal model for muscle-driven simulation of human gait. IEEE Trans. Biomed. Eng. 63, 2068–2079. https://doi.org/10.1109/TBME.2016.2586891.

Rasske, K., Thelen, D.G., Franz, J.R., 2017. Variation in the human Achilles tendon moment arm during walking. Comput. Methods Biomech. Biomed. Engin. 20, 201–205. https://doi.org/10.1080/10255842.2016.1213818.

Reber, L., Perry, J., Pink, M., 1993. Muscular control of the ankle in running. Am. J. Sports Med. 21 (6), 805–810.

Ross, S.A., Wakeling, J.M., 2016. Muscle shortening velocity depends on tissue inertia and level of activation during submaximal contractions. Biol. Lett. 12, 10–13. https://doi.org/10.1098/rsbl.2015.1041.

Seth, A., Hicks, J.L., Uchida, T.K., Habib, A., Dembia, C.L., Dunne, J.J., Ong, C.F., DeMers, M.S., Rajagopal, A., Millard, M., Hamner, S.R., Arnold, E.M., Yong, J.R., Lakshmikanth, S.K., Sherman, M.A., Ku, J.P., Delp, S.L., 2018. OpenSim: simulating musculoskeletal dynamics and neuromuscular control to study human and animal movement. PLoS Comput. Biol. 14 https://doi.org/10.1371/journal.pcbi.1006223.

Wang, Y., Weidner, N.J., Baxter, M.A., Hwang, Y., Kaufman, D.M., Sueda, S., 2019. RedMax: efficient & flexible approach for articulated dynamics. ACM Trans. Graph. 38 (4), 1–10.

Wang, Y., Verheul, J., Yeo, S.-H., Kalantari, N.K., Sueda, S., 2022. Differentiable Simulation of Inertial Musculotendons. ACM Trans. Graph. 41, 1–11. https://doi.org/10.1145/3550454.3555490.

Ward, S.R., Eng, C.M., Smallwood, L.H., Lieber, R.L., 2009. Are current measurements of lower extremity muscle architecture accurate? Clin. Orthop. Relat. Res. 467, 1074–1082. https://doi.org/10.1007/s11999-008-0594-8.

Xu, J., Chen, T., Zlokapa, L., Foshey, M., Matusik, W., Sueda, S., Agrawal, P., 2021. An end-to-end differentiable framework for contact-aware robot design. Proc. Robot. Sci. Syst. https://doi.org/10.15607/RSS.2021.XVII.008.

Zajac, F.E., 1989. Muscle and tendon: properties, models, scaling, and application to biomechanics and motor control. Crit. Rev. Biomed. Eng. 17, 359–411.